Journal of Molecular Spectroscopy xxx (2014) xxx–xxx

Contents lists available at ScienceDirect

Journal of Molecular Spectroscopy

journal homepage: www.elsevier.com/locate/jms

Electronic absorption spectra of linear C_6Br and C_6Br^+ in neon matrices

Karol Filipkowski, Jan Fulara, John P. Maier *

Department of Chemistry, University of Basel, Klingelbergstrasse 80, CH-4056 Basel, Switzerland

ARTICLE INFO

Article history:
Available online xxxx

Keywords:
Matrix isolation
Electronic spectra
CASPT2 and SAC-CI
C_6Br and C_6Br^+
Mass-selection

ABSTRACT

Electronic absorption spectra of linear C_6Br^+ and C_6Br have been recorded in 6 K neon matrices. Two strong absorption systems starting at 555.1 nm and 539.3 nm are assigned to the $1\,^2\Pi \leftarrow X\,^2\Pi$ electronic transition of C_6Br, and $1\,^3\Sigma^- \leftarrow X\,^3\Sigma^-$ of C_6Br^+. Excitation of normal modes along with overtones and combination bands in the excited electronic state are observed. Assignments are based on mass-selection, photobleaching behavior, comparison with the known electronic transitions of linear C_6Cl and C_6Cl^+, and excitation energies obtained with CASPT2 and SAC-CI theory as well as on computed vibrational frequencies.

1. Introduction

A number of substituted carbon chains and their ions have been studied by theoreticians and experimentalists due to their established presence in interstellar medium [1,2]. In contrast relatively little is known about their halogenated derivatives. Electronic absorption spectra of FC_6F^+, HC_6F^+ and C_nCl (n = 3-6), chains and their cations, were studied in neon matrices [3–5]. No spectroscopic data concerning bromine terminated carbon chains are available to date, and this paper fills this gap by presenting electronic absorption spectra of linear C_6Br and C_6Br^+ in 6 K neon matrices.

The mass-selection shows that the absorbing species are C_6Br or C_6Br^+, and the cations or neutral species are distinguished by the behavior of the systems on UV irradiation. There are a number of possible isomers, hence theory is required to decide which structures are the absorbers. To do this CASPT2 and SAC-CI calculations of the electronic excitation energies, and vibrational frequencies have been carried out. These data, as well as the previous studies on linear C_6H^+ and C_6Cl^+, allow the absorbing isomers to be identified.

2. Experimental

The experimental approach combines mass selection with matrix isolation. Cations were produced in a hot-cathode discharge source from a mixture of helium buffer gas and vapor of hexabromobenzene. The ions were extracted from the source, deflected by 90° to remove neutral species, and then selected by a quadrupole mass spectrometer. A resolution of unity gave a C_6Br^+ current of ~5 nA. Ions were co-deposited with either pure neon, or with addition of chloromethane, on the rhodium-coated sapphire plate. After 3 h of deposition ~100 μm thick matrix was grown. Neutral species are produced efficiently when only neon is used. As the deposition progresses accumulation of cations leads to a buildup of space charge, and as a consequence ions are repelled from the matrix. Electrons are ejected from metal surfaces by the impinging positive species, and are electrostatically attracted to the matrix neutralizing trapped ions. By adding CH_3Cl in a ratio of ~1:40 000 to neon, conditions are created under which ions can be trapped efficiently. Chloromethane acts as an electron scavenger undergoing dissociative electron capture to produce Cl^-, which shield cations embedded in the solid neon.

Electronic absorption spectra were measured by directing broadband light parallel to the substrate surface resulting in an optical path length of ~2 cm. Transmitted light is focused on a multimode optical fiber bundle and guided into a 0.3 m spectrograph. Spectra were recorded in the 220–1100 nm range by two CCD cameras. Subsequently the matrix was irradiated by photons below 260 nm from a medium pressure mercury lamp leading to detachment of electrons from Cl^-. These combine with the trapped cations, enhancing the absorptions of neutrals.

3. Results and discussion

3.1. Observations

The absorption spectrum recorded after deposition of mass selected C_6Br^+ ions in a 6 K neon matrix is shown in trace **b** (black trace) of Fig. 1. It reveals two absorption systems in the visible. The stronger one with onset at 555.1 nm shows a vibrational

* Corresponding author.

http://dx.doi.org/10.1016/j.jms.2014.10.006
0022-2852/

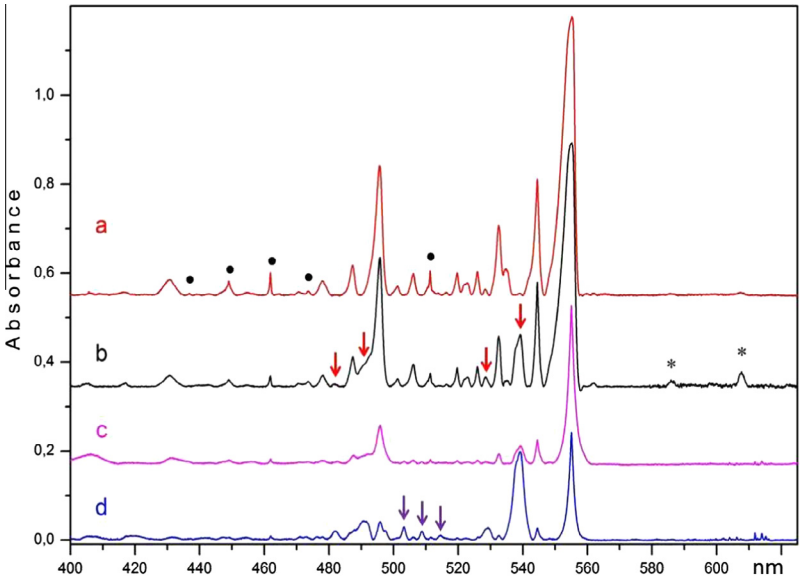

Fig. 1. Overview of the absorption spectra recorded after deposition of mass selected C_6Br^+ ions in pure neon at 6 K (trace **b**) and after subsequent photo-bleaching with a medium pressure mercury lamp (trace **a**). Trace **d** was observed after deposition in neon including a trace of CH_3Cl, and after irradiation (trace **c**). Absorption of fragmentation products are indicated. Absorptions of $\mathbf{C}_6$ are identified with • and those of $\mathbf{C}_6^-$ by ∗.

progression in the 550-440 nm range. The second system has a simpler appearance, with bands at 539.3, 529.3, 490.4 and 482.0 nm (red[1] arrows, Fig. 1). Trace **a** shows the spectrum recorded after irradiation of the matrix with photons <260 nm. Spectroscopic features located in the visible gain intensity, proving their neutral origin. Hence they are assigned to an electronic transition of C_6Br isomers because of the mass-selection. The four bands comprising second system vanished and are attributed to a C_6Br^+ structure. The two weak features at 539.3 and 529.3 nm in trace **a** are due to the overlap of weak bands of C_6Br and C_6Br^+.

The other two traces in Fig. 1 show electronic absorptions of mass selected C_6Br^+ recorded after deposition in neon premixed with a trace of CH_3Cl (trace **d**), and after subsequent irradiation with a mercury lamp (trace **c**). A substantial difference between traces **b** and **d** is apparent, illustrating how the concentration ratio of cations to neutrals in the matrix can be manipulated by addition of an electron scavenger. An absorption system of neutral C_6Br commencing at 555.1 nm is again present. However this time the absorptions are weaker even though the deposited ion current of C_6Br^+ was comparable in both cases. On the other hand the four bands assigned to C_6Br^+ become stronger. Other bands that decrease in intensity upon irradiation are evident in trace **d** (magenta arrows). These lie at 514.6, 508.8, and 503.2 nm, and their behavior points toward a cationic origin, a part of the C_6Br^+ system.

The bands located at 511.3 and 461.9 nm (Fig. 1) belong to the $^3\Sigma_u^- \leftarrow X\,^3\Sigma_g^-$ transition of C_6 [6]. Additional bands of this system are seen at 473.6, 449.1 and 436.9 nm, marked with • in trace **a**. The C_6 molecules are produced by collision induced cleaving of the C–Br bond during C_6Br^+ deposition. In contrast the known bands [7] of l-C_6^+ were not detected and this can be attributed to effective neutralization of cationic species during deposition by electrons liberated from surfaces of the chamber. In the absence of an electron scavenger, products of C_6Br^+ fragmentation can recombine with electrons to form anions. Such an anionic system due to the $^2\Pi_u \leftarrow X\,^2\Pi_g$ transition of l-C_6^- (marked with ∗) with onset at 607.6 nm is present in trace **b**. Upon irradiation it disappears whereas the C_6 absorption system gains in intensity (trace **a**). Formation of anionic fragmentation products is not observed when depositing in CH_3Cl doped neon (traces **c** and **d**) because the electrons are trapped as Cl^-. Bands assigned to C_6 are also present in traces **c** and **d**; however their intensity does not change after bleaching with photons below 260 nm, indicating that detachment of electrons from C_6^- is the sole process leading to increase in intensity of the neutral C_6 system in trace **a**.

There are additional weaker absorption systems in the UV not shown in Fig. 1, and two of them show a distinct vibrational progression. One with origin band at 345 nm diminishes upon irradiation with a mercury lamp, and is thus expected to be an absorption of C_6Br^+. This band is also present in a matrix containing chloromethane and weakly in the spectrum recorded after irradiation, providing support for the assignment to a cationic species. The second system with onset at 317.5 nm gains in intensity after photobleaching, and a vibrational progression in the 315-265 nm range becomes apparent. Such a behavior points towards a neutral carrier. This band system is not present after deposition in a matrix containing chloromethane but the sharp feature at 355.9 nm is seen. It becomes stronger after irradiation and an additional weak band, blue shifted by 245 cm^{-1}, becomes visible. The pattern indicates that experiments with or without chloromethane create conditions under which different isomers of C_6Br, C_6Br^+ and possible fragmentation products are formed.

3.2. Computations

Geometries of ten plausible isomers of C_6Br and C_6Br^+ were initially chosen for *ab initio* calculations. The ground state geometries where calculated using the B3LYP exchange-correlation functional [8] combined with 6-311++G(3df,p) basis set, [9] and the Gaussian 09 program [10]. Harmonic vibrational frequencies were calculated to assure that the structures correspond to a minimum on the potential energy surface. The five energetically lowest lying isomers shown in Chart 1 were selected for a further refinement. Their geometries were recalculated using the second-order Möller–Plesset [11] perturbation method with a correlation-consistent (cc-pVTZ) basis set [12], followed by calculation of vibrational frequencies. Zero point energy corrections were included.

[1] For interpretation of color in Fig. 1, the reader is referred to the web version of this article.

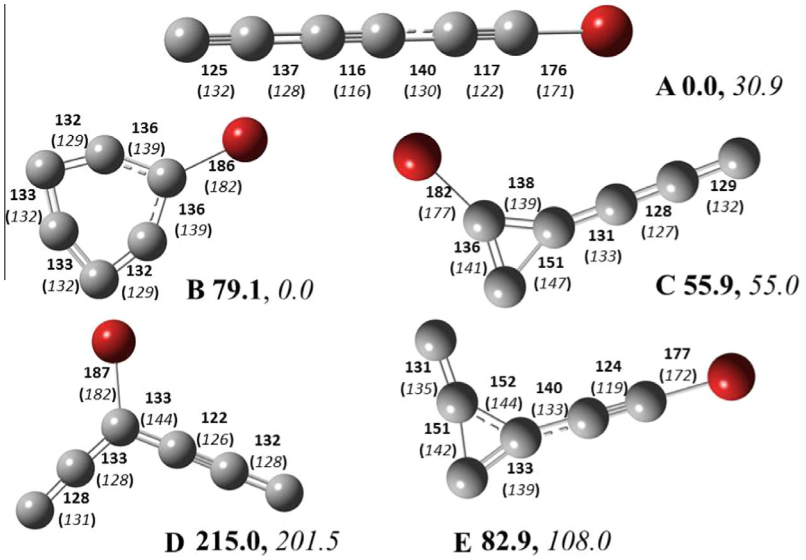

Chart 1. Structures (pm), and relative ground state energies (kJ/mol) of the five energetically lowest isomers of C_6Br (bold) and C_6Br^+ (italic), optimized at MP2 level of theory with a cc-pVTZ basis set including a zero point energy correction.

These structures served as the starting point for calculation of vertical excitation energies using second-order perturbation theory CASPT2 implemented in the MOLCAS program [13] The active space was build from 11 electrons and 11 orbitals in case of the neutrals and 10 electrons in 10 orbitals for the cations. Additionally "Symmetry Adopted Cluster – Configuration Interaction" (SAC-CI) [14,15] calculations were carried out to aid the identification of the isomers responsible for the observed electronic transitions. The excitations energies together with the transition oscillator strengths are given in Table 2 for C_6Br and Table 3 for C_6Br^+.

The most stable structure among C_6Br neutral species is the linear isomer **A**, followed by isomer **C** lying 56 kJ mol^{-1} higher in energy. The structure with a six-membered ring and an exocyclic bromine atom, C_{2v} symmetry, is ~79 kJ mol^{-1} above the linear species. The two highest lying isomers **E** and **D** are 83 and 215 kJ mol^{-1} above **A**. The most stable among cationic species is cyclic $\mathbf{B^+}$, whereas the linear one $\mathbf{A^+}$ lies 31 kJ mol^{-1} above it. Triplet ground state is predicted for $\mathbf{A^+}$, whereas $\mathbf{B^+}$, $\mathbf{C^+}$, $\mathbf{D^+}$ and $\mathbf{E^+}$ are singlets.

The absorption system in the visible is shown in more detail in Fig. 2. Trace **a** was recorded after deposition of mass-selected C_6Br^+ ions. Trace **b** was recorded after irradiation with <260 nm photons. Isomer **B** possesses an electronic transition at 2.37 eV f = 0.003

Table 1
Absorption bands (±0.2 cm^{-1}) in the electronic spectrum of linear C_6Br and C_6Br^+ in a 6 K neon matrix and the suggested vibrational assignments.

Species	λ (nm)	$\tilde{\nu}$ (cm^{-1})	$\Delta\tilde{\nu}$ (cm^{-1})	Assignment
l-C_6Br	555.1	18015	0	0_0^0 $\mathbf{1}\,^2\Pi \leftarrow X\,^2\Pi$
	548.2	18224	210	$13_0^1 15_0^1$
	544.5	18366	351	6_0^1
	538.9	18555	541	$11_0^2/12_0^2$
	534.9	18695	681	6_0^2
	532.4	18783	768	5_0^1
	528.4	18925	910	10_0^2
	525.9	19015	1000	$5_0^1 13_0^1 15_0^1$
	522.5	19139	1124	$5_0^1 6_0^1$
	519.7	19242	1227	4_0^1
	516.3	19369	1354	$5_0^1 6_0^1 13_0^1 15_0^1$
	511.3	19560	1545	$4_0^1 6_0^1$
	506.1	19759	1744	$5_0^1 12_0^2/5_0^1 12_0^2$
	501.2	19952	1937	3_0^1
	495.7	20174	2159	$1_0^1/2_0^1$
	487.3	20521	2507	$1_0^1 6_0^1/2_0^1 6_0^1$
	477.9	20925	2910	$1_0^1 5_0^1/2_0^1 5_0^1$
	473.6	21115	3100	$1_0^1 5_0^1 6_0^1/2_0^1 5_0^1 6_0^1$
l-C_6Br^+	539.3	18543	0	0_0^0 $\mathbf{1}\,^3\Sigma^- \leftarrow X\,^3\Sigma^-$
	529.3	18893	350	6_0^1
	514.6	19433	890	8_0^2 or 9_0^2
	503.2	19873	1330	4_0^1
	490.4	20392	1849	3_0^1
	486.2	20569	2026	2_0^1
	482.0	20747	2204	$3_0^1 6_0^1$

Calculated stretching modes frequencies (cm^{-1}) in the ground electronic state; l-C_6Br: ν_1 = 2156, ν_2 = 2111, ν_3 = 1905, ν_4 = 1287, ν_5 = 802, ν_6 = 345; l-C_6Br^+: ν_1 = 2110, ν_2 = 2071, ν_3 = 1810, ν_4 = 1308, ν_5 = 827, ν_6 = 358.

Table 2
Vertical excitation energies and oscillator strengths of C_6Br isomers calculated with CASPT2 and SAC-CI and cc-pVTZ basis set.

Isomer	State	CASPT2		SAC-CI	
		eV	f	eV	f
A	$X^2\Pi$	0		0	
	$1^2\Pi$	2.78	0.06	2.77	0.004
	$2^2\Pi$	4.48	0.0004	4.61	0.006
	$3^2\Pi$	4.64	0.05		
	$4^2\Pi$	5.08	0.0001		
	$1^2\Sigma^+$	5.59	0.007		
B	X^2A'	0		0	
	$1^2A'$	1.62	0.003	2.60	0.008
	$2^2A'$	1.73	0.001		
	$3^2A'$	2.37	0.003		
C	X^2A''	0		0	
	$1^2A''$	2.39	0.009	3.35	0.05
	$2^2A''$	2.49	0.007	5.04	0.001
	$3^2A''$	3.41	0.04		
	$4^2A''$	4.48	0.001		
D	X^2A''	0		0	
	$1^2A''$	2.14	0.006	2.60	0.02
	$2^2A''$	2.31	0.008	4.28	0.005
	$3^2A''$	2.39	0.003		
	$4^2A''$	3.71	0.045		
	$5^2A''$	4.34	0.024		
E	X^2A''	0		0	
	$1^2A''$	3.42	0.024	3.48	0.08
	$2^2A''$	3.84	0.005	5.55	0.04
	$3^2A''$	3.91	0.002		
	$4^2A''$	4.42	0.02		

Table 3
Vertical excitation energies and oscillator strengths of C_6Br^+ isomers calculated with CASPT2 and SAC-CI and cc-pVTZ basis set.

Isomer	State	CASPT2		SAC-CI	
		eV	*f*	eV	*f*
A$^+$	$X\,^3\Sigma^-$	0		0	
	$1\,^3\Sigma^-$	2.83	0.003	2.61	0.31
	$2\,^3\Sigma^-$	3.03	0.002	4.07	0.15
	$3\,^3\Sigma^-$	3.61	0.02	4.54	0.05
B$^+$	$X\,^1A_1$	0		0	
	$1\,^1B_2$	3.46	0.01	3.22	0.05
	$2\,^1B_2$	5.24	0.04	3.71	0.003
	$3\,^1B_2$	5.69	0.02	5.82	0.02
	$1\,^1B_1$	2.39	0.002	1.56	0.001
C$^+$	$X\,^1A'$	0		0	
	$1\,^1A'$	2.19	0.13	2.12	0.18
	$2\,^1A'$	3.51	0.43	3.55	0.04
	$3\,^1A'$	3.64	0.17	3.74	0.27
	$4\,^1A'$	4.61	0.06	4.42	0.2
	$5\,^1A'$	5.11	0.01	4.73	0.03
D$^+$	$X\,^1A'$	0		0	
	$1\,^1A'$	1.46	0.001	2.51	0.01
	$2\,^1A'$	2.15	0.07	3.31	0.02
	$3\,^1A'$	2.64	0.0001	3.38	0.12
	$4\,^1A'$	3.04	0.12	3.95	0.08
	$5\,^1A'$	3.44	0.01	4.50	0.07
E$^+$	$X\,^1A'$	0		0	
	$1\,^1A'$	2.22	0.34	2.43	0.06
	$2\,^1A'$	2.35	0.03	4.03	0.25
	$3\,^1A'$	4.17	0.17	4.37	0.17
	$4\,^1A'$	4.42	0.08	4.95	0.06
	$5\,^1A'$	5.05	0.007	5.68	0.09

(CASPT2), 2.60 eV $f = 0.008$ (SAC-CI), close to the onset of the C_6Br system at 555.1 nm (2.23 eV). Transitions at 1.62 eV and 1.73 eV with oscillator strengths of 0.0029 and 0.0008, are predicted for the **B** cyclic structure, excluding it as the carrier. Two higher energy C_6Br isomers **C**, and **D** are also excluded, as they possess more than one transition near the 555.1 nm system. CASPT2 calculations predict the strongest electronic transition for linear **A** at 2.78 eV with $f = 0.06$ close to the experimental value. A similar value 2.77 eV was obtained by SAC-CI calculations, though with $f = 0.004$. In comparison the $^2\Pi \leftarrow X\,^2\Pi$ transition of l-C_6H lies at 530 nm, and 545.8 nm for l-C_6Cl. This electronic transition involves predominately electronic excitations within a bonding π-delocalized network of a carbon chain. Introduction of terminal halogen atom stabilizes σ-orbitals, with only little effect on the carbon π-orbitals.

In view of the calculations and similarity to the absorption of l-C_6H and l-C_6Cl, the 555.1 nm system (Fig. 2) is assigned to the $1\,^2\Pi \leftarrow X\,^2\Pi$ transition of linear C_6Br, isomer **A**. Analysis of the vibrational structure provides support for this. The strong band to higher energy of the origin involves the excitation of the ν_6 stretching mode, the C–Br bond, and the frequency 350.7 cm^{-1} is in accord with the value 345 cm^{-1} calculated for the ground electronic state (Table 1). An overtone of this mode is observed ~ 680 cm^{-1} above the origin. The three bands that lie 768, 1227 and 1937 cm^{-1} to higher energy of 0_0^0 transition are assigned to the ν_5, ν_4 and ν_3 totally symmetric stretching C–C modes (Footnote Table 1). The strongest band in the lower panel of Fig. 2 is 2159 cm^{-1} above the 0_0^0 band in energy. B3LYP calculations of harmonic vibrational frequencies predict two transitions close to this value; excitation of ν_2 at 2111 cm^{-1} and ν_1 at 2156 cm^{-1}. In addition, combination bands and overtones are discernible in the spectrum.

The upper trace in Fig. 3 shows the absorption spectrum recorded after deposition of mass-selected C_6Br^+ in neon (upper trace) including a small amount of CH_3Cl. Middle trace was recorded after subsequent UV irradiation. Bottom trace is the difference between the upper two, expanded by a factor of 2, and peaks that point downward are the absorptions of C_6Br^+. The onset of the cationic system is at 539.3 nm (2.30 eV). Theory predicts for the global minimum structure **B**$^+$ a moderately strong $1\,^1A_1 \leftarrow X\,^1B_2$ transition at 3.46 eV (CASP2), 3.22 eV (SAC-CI), far away from the observations. Higher energy isomers **C**$^+$, **D**$^+$ and **E**$^+$ can be also excluded. They possess more than one transition in this region; besides their vibrational frequencies do not match the observed pattern. Thus only the linear isomer **A**$^+$ is an acceptable candidate as the carrier of the 539.3 nm system. The vertical excitation energy calculated with MS-CASPT2 2.83 eV is 0.53 eV higher

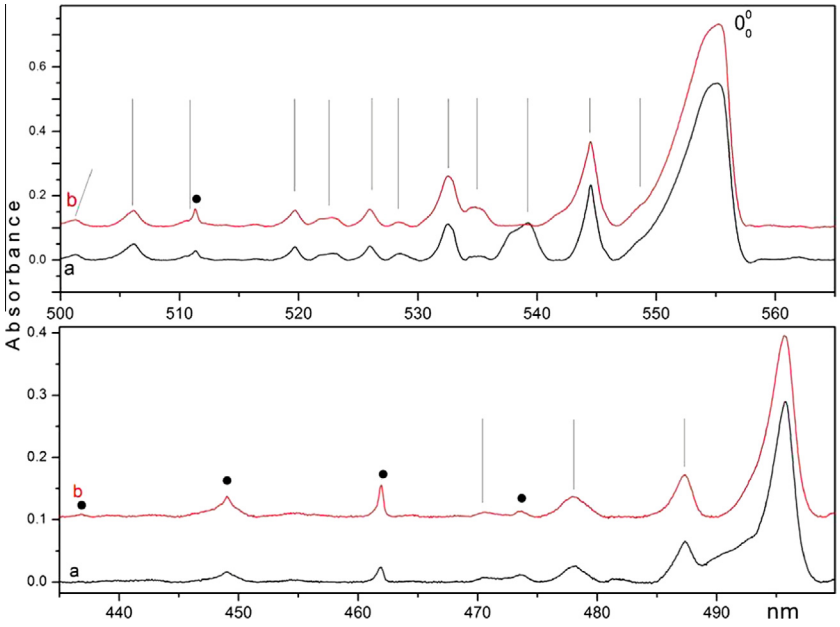

Fig. 2. Electronic absorption spectrum of the $1\,^2\Pi \leftarrow X\,^2\Pi$ transition of linear C_6 Br recorded after deposition of mass selected $m/z = 151$ cations in 6 K neon matrix (trace **b**), and after subsequent irradiation with <260 nm photons (trace **a**). The absorption system of neutral l-C_6 is present because of fragmentation during matrix growth. Bands belonging to l-C_6Br system are identified with vertical lines and their frequencies are given in Table 1. Absorptions of C_6 are indicated by •.

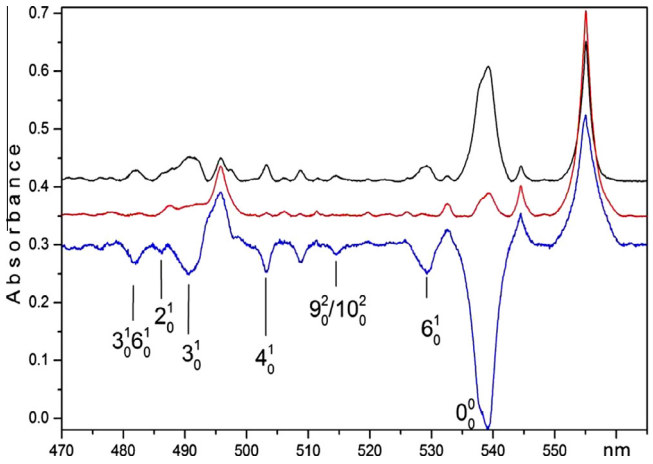

Fig. 3. Electronic absorption spectrum of linear C_6Br^+ recorded after deposition of mass selected cations (m/z = 151) in a 6 K neon matrix containing a trace of CH_3Cl (black trace). Red trace was observed after irradiation of matrix with <260 nm photons. Blue trace is the difference between the upper two traces, expanded by 2. Peaks pointing down diminished after UV exposure and are assigned to the $\mathbf{1}^3\Sigma^- \leftarrow X^3\Sigma^-$ transition of linear C_6Br^+. (For interpretation of the references to color in this figure legend, the reader is referred to the web version of this article.)

than the observation. Furthermore the $X^3\Sigma^-$ ground electronic state of linear $\mathbf{A}^+$ has the same symmetry as for the l-C_6H^+ and l-C_6Cl^+ species with known $^3\Sigma^- \leftarrow X^3\Sigma^-$ electronic transitions, displaced 23.5 and 11.9 nm from the observed origin of C_6Br^+. Hence the system shown in Fig. 3 is assigned to the $1^3\Sigma^- \leftarrow X^3\Sigma^-$ transition of linear C_6Br^+, $\mathbf{A}^+$. Comparison of the vibrational progression pattern with calculated harmonic frequencies for $X^3\Sigma^-$ (Footnote Table 1) supports the assignment. Band 358 cm^{-1} to higher energy of the origin corresponds to the C–Br bond stretch excitation. The slightly higher frequency than for linear C_6Br is a reflection of the ground state geometries. The C–Br bond distance in the cation (171 pm) is smaller than in C_6Br (176 pm). The ground state configuration for C_6Br is $X^2\Pi...5\pi^4 20\sigma^2 6\pi^4 7\pi^3$ and the observed transition involves $6\pi^4 \rightarrow 7\pi^3$ electronic excitation. For C_6Br^+, $X^3\Sigma^-$ the electronic excitation is $6\pi^4 \rightarrow 7\pi^2$. Consequently the electronic transitions of l-C_6Br and l-C_6Br^+ are expected to be close in energy; the observed difference is 15.8 nm.

In conclusion, this article presents the electronic $1^3\Sigma^- \leftarrow X^3\Sigma^-$ and $1^2\Pi \leftarrow X^2\Pi$ absorption spectra of linear C_6Br and linear C_6Br^+ for the first time. This in turn provides the means of identification of such species in situ, via their electronic transitions, and opens the way to gas phase studies.

Acknowledgment

This work was supported by the Swiss National Science Foundation (Project 200020-124349/1).

References

[1] M. Guélin, J. Cernicharo, M. Travers, M.C. McCarthy, Astron. Astrophys. 317 (1997) L1–L4.
[2] J. Cernicharo, M. Guélin, Astron. Astrophys. 309 (1996) L27–L30.
[3] K. Filipkowski, J. Fulara, J.P. Maier, Int. J. Mass Spectrom. 354–355 (2013) 188–192.
[4] J. Van Wijngaarden, A. Batalov, I. Shnitko, J. Fulara, J.P. Maier, J. Phys. Chem. 108 (2004) 4219–4223.
[5] J. Van Wijngaarden, I. Shnitko, A. Batalov, P. Kolek, J. Fulara, J.P. Maier, J. Phys. Chem. 109 (2005) 5553–5559.
[6] D. Forney, J. Fulara, P. Freivogel, M. Jakobi, D. Lessen, J. Chem. Phys. 103 (2005) 48–53.
[7] J. Fulara, E. Riaplov, A. Batalov, I. Shnitko, J.P. Maier, J. Chem. Phys. 120 (2004) 7520–7525.
[8] C. Lee, W. Yang, R.G. Parr, Phys. Rev. B 37 (1988) 785–789.
[9] T. Clark, J. Chandrasekhar, G.W. Spitznagel, P.v.R. Schleyer, J. Comput. Chem. 4 (1983) 294–301.
[10] Gaussian 09, Revision D.01, M.J. Frisch, G.W. Trucks, H.B. Schlegel, G.E. Scuseria, M.A. Robb, J.R. Cheeseman, G. Scalmani, V. Barone, B. Mennucci, G. Petersson, et al. Gaussian Inc., Wallingford, CT, 2009.
[11] C. Møller, M.S. Plesset, Phys. Rev. 46 (1934) 0618–0622.
[12] T.H. Dunning Jr., J. Chem. Phys. 90 (1989) 1007–1023.
[13] F. Aquilante, L. De Vico, N. Ferré, G. Ghigo, P.-Å. Malmqvist, P. Neogrády, T.B. Pedersen, M. Pitonak, M. Reiher, B.O. Roos, L. Serrano-Andrés, M. Urban, V. Veryazov, R. Lindh, J. Comput. Chem. 31 (2010) 224.
[14] H. Nakatsuji, K. Hirao, J. Chem. Phys. 68 (1978) 2053–2065.
[15] H. Nakatsuji, Chem. Phys. Lett. 67 (1979) 329–333.